THE JOURNAL OF PHYSICAL CHEMISTRY C

pubs.acs.org/JPCC Article

# Oscillatory Behavior in Cobalt Electrodeposition with 3-Mercapto-1-Propanesulfonate

Y. Hu and Q. Huang*

Cite This: J. Phys. Chem. C 2020, 124, 21608−21616 Read Online

ACCESS | Metrics & More | Article Recommendations | Supporting Information

**ABSTRACT:** A potential oscillation was observed during galvanostatic deposition of Co in the presence of 3-mercapto-1-propanesulfonate (MPS) and a systematic study was conducted. A suppression effect on Co deposition by MPS was seen in cyclic voltammetry (CV) and such effect was not affected by pH. To fully understand the suppression effect and oscillation mechanism, several influencing factors in the galvanostatic process such as pH, $Co^{2+}$ and MPS concentrations, agitation, and a buffer agent were thoroughly investigated. Moreover, mercaptopropionic acid, an alternative additive with a similar molecular structure as MPS, was used to determine the roles of thiol and sulfonate groups during the oscillation. Based on the experiment results, a kinetically controlled mechanism including a potential-dependent adsorption−desorption of the Co−MPS complex accompanied by the accumulation and dissolution of $Co(OH)_2$ was proposed.

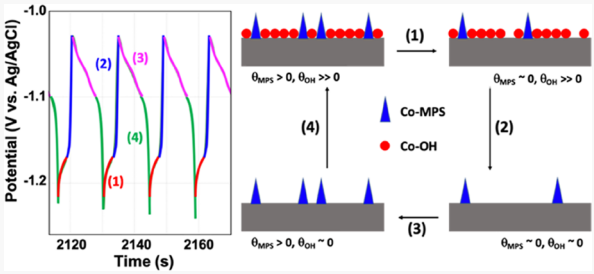


## INTRODUCTION

The damascene copper/low-k interconnect scheme has been used ubiquitously in semiconductor integrated circuits but are continuously facing difficulties in achieving defect-free Cu filling as the dimension of interconnect structures continues to decrease.[1] More importantly, the exponential increase of Cu resistivity as the dimension falls below the electron mean free path of Cu results in the greater RC delay,[2,3] jeopardizing the performance gain earned from device innovations. Therefore, metals with shorter electron mean free path, such as cobalt (Co), have been explored as an alternative conductor. There are two main advantages in Co: (i) the relatively high melting point of Co is advantageous for electromigration; (ii) despite a higher bulk resistivity, Co shows a lower resistivity than Cu when the critical dimension of feature is approaching or smaller than Cu electron mean free path (about 38 nm).[4]

Organic additives are used in damascene Cu chemistries not only to achieve void-free metal filling process but also to control the impurity incorporation and grain structures of deposited Cu.[5−7] The former is achieved as a result of the interplay between multiple additive components.[8] The metal cation reduction kinetics are thus altered upon various mechanisms, such as an interaction between metal cations and additives in bulk electrolytes,[9] the adsorption, desorption, and breakdown of a catalytic or inhibitive intermediate species adsorbed on the electrode surface,[10] or competitive adsorption between multiple intermediates on the electrode surface.[11,12] These mechanisms at certain conditions can trigger electrochemical oscillation, where either the potential or current changes periodically within a certain range during galvanostatic or potentiostatic deposition, respectively. Electrochemical oscillation phenomena in general have been reported in various systems,[13−17] where an autocatalytic reaction leads to a positive feedback loop. They can be classified based on the role of double-layer potential, whether it is a nonessential component in a purely chemical autocatalytic loop, or is a slow-changing factor with its effect gradually accumulating and eventually triggering an abrupt change of the direction of the autocatalytic reaction, or even forms the autocatalytic loop itself.[18]

Among damascene Cu chemistries, oscillation processes have also been reported. For most additive-containing cases, oscillation has been attributed to polarization curves that contain a region of negative differential resistance (NDR), where the current decreases with the increasing driving force.[14,19,20] The extremely rapid (autocatalytic) self-breakdown kinetics of a suppressor−accelerator complex molecule conjugated through a cuprous ion, together with the slow kinetics of the formation and accumulation of such a complex on the electrode surface, constructs the key elements of the oscillation. This chemical oscillation on the electrode surface was manifested through the electrochemical deposition of copper, where the different surface adsorbates change the reduction kinetics of copper, resulting in electrochemical oscillation. However, NDR is not a requirement for Cu oscillation in additive-containing chemistries. For example, Cu

Received: July 27, 2020
Revised: September 8, 2020
Published: September 10, 2020

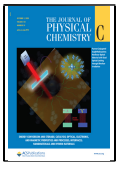







https://dx.doi.org/10.1021/acs.jpcc.0c06877
J. Phys. Chem. C 2020, 124, 21608−21616

oscillation occurred upon the addition of benzyl viologen and bis (3-sulfopropyl)disulfide (SPS), where NDR was not observed in the cyclic voltammetry (CV) curves.[21] Studies using a rotating ring-disk electrode suggested that the oscillation process is related to the potential-dependent adsorption and desorption of two different additives, while such processes can also be mediated by cuprous ions as other studies suggest. In addition, the Cu oscillation process was also reported in a simple electrolyte with complexing carboxyl acid, such as lactate and tartrate, where nanoscale multilayers or a mixture between Cu and $Cu_2O$ can be formed.[15,22,23]

Although Cu oscillation has been well studied, oscillation during Co electrodeposition with additives has not been reported. The only oscillatory Co deposition, to the best of our knowledge, was reported during dendrite growth within a nanometric thin layer of an additive-free electrolyte.[24] The mass transport in this extremely thin configuration was confined as two-dimensional diffusion, which limits the supply of the Co cation and results in potential variation during galvanostatic deposition in that report. In this paper, potential oscillation is reported for Co electrodeposition in an electrolyte containing 3-mercapto-1-propanesulfonate (MPS), the monomer version of the commonly used dimer accelerator, SPS. MPS is of interest to Co deposition as its adsorption and incorporation enable the tuning of impurity and control of the grain structure of electrodeposited Co. The effects of the critical parameters including pH, $Co^{2+}$, and MPS concentrations, as well as agitation, on the oscillation are systematically investigated here. Mercaptopropionic acid (MPA), a carboxyl acid with a similar molecular structure as MPS, is used to dissect the roles the thiol and sulfonate groups play. A competitive adsorption mechanism is proposed to explain the observations.

## METHODS

A traditional three-compartment electrochemical cell was used for the experimental studies, where the catholyte and anolyte are separated by a glass frit. A saturated Ag/AgCl electrode (0.197 V vs normal hydrogen electrode (NHE)) was used as the reference electrode, and all potentials were referred to this electrode in this paper. The reference electrode compartment is connected to the catholyte through a capillary. The counter electrode was a Co foil (purity at least 99.96%) with a surface area much larger than the cathode. The platinum (Pt) rotating disk electrode (RDE) was used as the cathode and the deposition area is 0.196 $cm^2$. Pt RDE is typically stripped and cleaned after use before storage. It was therefore typically used as is for the next study only after 1 M $H_2SO_4$ clean and DI water rinse.

The Co electrolytes at various concentrations of $CoSO_4$ were used in the studies. The solution pH was adjusted with $H_2SO_4$ and NaOH. Concentrated MPS solution (17 800 ppm, or 0.1 M), concentrated mercaptopropionic acid (MPA) solution (10 614 ppm, or 0.1 M), and boric acid ($H_3BO_3$, 0.4 M) were prepared by dissolving the corresponding chemicals in water. Calculated amounts of the concentrate were then added into the Co makeup solution up to various final concentrations. All salts and organic additives were at least ACS grade and used as received. Deionized (DI) water with a resistivity of 18.2 MΩ cm was used in all studies. An Autolab 302N potentiostat with a frequency analyzer was used for all electrochemical studies. The impedance spectra were acquired using a 10 mV sinusoidal potential wave with frequency from 100 kHz to 100 mHz. An Apreo scanning electron microscope (SEM) was used to characterize the morphology of the electrodeposited Co films.

## RESULTS AND DISCUSSION

**Cyclic Voltammetry.** Figure 1 shows the cyclic voltammetry (CV) of Co electrodeposition on the Pt electrode at two

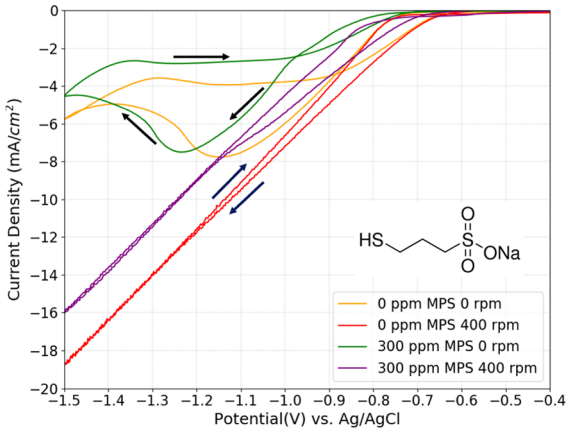


**Figure 1.** Cyclic voltammetry of Co electrodeposition on Pt RDE at different rotation rates in 0.05 M Co solutions with different MPS concentrations at pH = 4. Scan rate = 20 mV/s.

different rotation rates, where a suppression effect of MPS was observed. The electrolyte comprised 50 mM $CoSO_4$, the scan rate was 20 mV/s, and the pH was adjusted to 4. Co deposition started at around −0.70 V in the absence of the additive and rotation. As the potential reached more negative than −1.1 V, the depletion of $Co^{2+}$ caused a decrease of the current density, a classic feature of stationary CV. Since the Pt electrode was not preplated with Co, Co deposition in the cathodic and anodic scans occurred on the Pt and Co surface, respectively, causing a crossover at −0.90 V on the reverse (anodic) sweep. Adding 300 ppm MPS into the electrolyte resulted in a suppression in Co deposition, where the magnitude of current density was always lower than the additive-free case in the kinetically controlled regime, i.e., the cathodic sweep before the peak. The crossover disappeared when a finite rotation rate, for example, 400 rpm, was applied, as the mass transport was facilitated by the rotation and the diffusion-limited current decay was eliminated. A similar suppression effect was also seen with MPS at 400 rpm, where a nearly constant potential shift was observed between the CVs with and without 300 ppm MPS. The study shown in Figure 1 was carried out at a pH of 4 and the same trend was also observed at other pH's studied, as shown in Figure S-1 in the Supporting Information. It is worth noting here that MPS was added as a sodium salt and no pH change was observed upon this addition. Therefore, the above observations are attributed to MPS rather than any side effects of pH change. In addition, the ohmic resistances of the electrolytes were measured with impedance spectroscopy, as shown in Figure S-2 in the Supporting Information. The CVs were not corrected with the ohmic drop to allow easy comparison with the potential transient reading in galvanostatic deposition. However, the addition of MPS only slightly lower the ohmic resistance; therefore, the suppression effect characterized as the potential drift in CV is indeed slightly underestimated.


https://dx.doi.org/10.1021/acs.jpcc.0c06877
J. Phys. Chem. C 2020, 124, 21608−21616

In our previous work, a class of dioxime molecules suppresses Co deposition through an adsorbed $Co^{2+}$−dioxime complex and this suppression breaks down as the cationic adsorbate is reduced and incorporated into the Co film as impurities.[25−27] This suppression breakdown results in a hysteresis in the CV curves, where the anodic sweep is of no difference from the additive-free case as the adsorbate is being incorporated. However, the suppression effect of MPS observed here is different, where the magnitude of current density is always lower than the additive-free case in the cathodic and anodic sweeps. Complex structures between metal cations and MPS or other sulfur-bearing compounds are not uncommon in the electrodeposition systems. For example, Hai et al.[19] proved the formation of the $H_2O$−Cu(I)−MPS complex, where the addition of MPS into the $Cu^{2+}$ solution led to a color change from blue to yellow, which directly correlated with the formation of Cu(I)−MPS complex. Moreover, it was reported that the thiol-terminated molecules could bond to the Co substrate to form a monolayer of the molecule.[28] In addition, secondary ion mass spectrometry (SIMS) analysis[29] showed that the addition of MPS caused a high incorporation of sulfur in the electrodeposited Co film and a lower content of nitrogen from dioxime. It is therefore believed that MPS could adsorb on the Co electrode surface and form the Co−MPS complex adsorbate through the thiol group. This adsorbate not only blocks the electrode surface and moderately slows the charge transfer but also gets incorporated into the Co film as impurities. In addition, because no pH buffer agent is present in the electrolyte, the pH near the electrode surface can rise significantly and $Co(OH)_2$ can be formed on the electrode surface when the potential is highly negative, namely, when hydrogen evolution reaction (HER) reaches its mass transport limit or when water reduction reaction starts. While the $Co(OH)_2$ adsorbate has indeed been proposed as an intermediate species in a two-step Co electrodeposition mechanism,[30] the formation of the excessive hydroxide adsorbate at a high surface pH is expected to block the electrode surface and completely prohibit metal deposition. It, therefore, is often avoided in film deposition. Nevertheless, either one of the two adsorbates, Co−MPS complex or $Co(OH)_2$, is believed to be sufficient for the kinetic suppression effect observed in the CVs.

**Chronopotentiometry—Influence of Current.** Figure 2 shows the potential transients during galvanostatic deposition of Co with the same electrolyte in Figure 1, with 50 mM $CoSO_4$ and pH of 4. The transients were acquired in a single experiment with multiple current steps. Three consecutive doses of 100 ppm MPS were added to the solution at 100, 200, and 300 s, respectively, as Co was deposited at −2.55 mA/cm$^2$ and 400 rpm. The addition of 300 ppm MPS caused a small decrease of the potential of about 100 mV, consistent with the suppression effect observed in the CV studies. Further increasing current density to −4.08 mA/cm$^2$ led to an oscillation in potential. The detailed oscillation curves were included as the inset in Figure 2. Upon the increase of current, the potential suddenly dropped to −1.08 V, followed by a rapid increase to −0.96 V. The potential oscillation gradually started afterward and remained within a range from −0.95 to −1.05 V. The frequency of this potential oscillation was as high as 0.3 Hz or 3.33 s per cycle based on the observation from 1100 to 1200 s. However, this oscillation was unstable at this condition, where it started at around 1130 s with a continuously diminishing amplitude and eventually disappeared after about 100 s. A steady-state potential of −0.99 V was obtained afterward. A stable oscillation was observed when the current was further increased to −6.12 mA/cm$^2$. The average potential at this current density, about −1.07 V, was about 80 mV more negative than that at −4.08 mA/cm$^2$. On the other hand, electrochemical impedance analysis (Figure S-2 in the Supporting Information) showed that the ohmic resistance of the electrolyte was about 180 Ω. An increase of current density from −4.08 to −6.12 mA/cm$^2$ on a 0.5 cm RDE translated to a potential shift of −72 mV. Therefore, the oscillations observed at these different current densities were believed to stem from the same electrochemical reactions at a same potential after the ohmic correction. Potential oscillation at a much higher current density of −12.76 mA/cm$^2$ seemed to be significantly inhibited, where the potential stayed at around −1.26 V for most of the time with sporadic "spikes" at a less negative potential of −1.20 V.

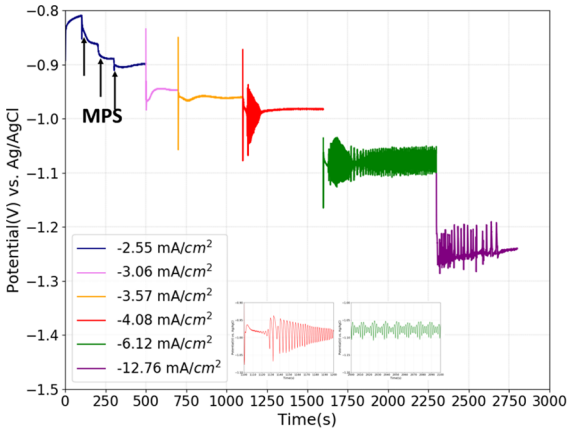


**Figure 2.** Potential transients for Co deposition at 400 rpm and different current densities in 0.05 M Co solutions with the addition of 300 ppm MPS at pH = 4. The detailed oscillation curves at -4.08 and -6.12 mA/cm$^2$ are shown in the inset.

**Chronopotentiometry—Influence of pH.** The influence of pH on Co deposition in the presence of MPS was studied. Figure 3a shows the potential transients during galvanostatic deposition of Co at a fixed rotation of 400 rpm in an electrolyte with 50 mM $CoSO_4$ and a pH of 3. Similar to the previous study, three doses of 100 ppm MPS were consecutively added into the Co solution at 250, 350, and 450 s with the current density kept at a constant of −2.55 mA/cm$^2$. Based on the pH measurement, the addition of 300 ppm MPS did not change the pH of the $Co^{2+}$ solution. The galvanostatic study showed that the addition of MPS caused depolarization at a low current density, which was opposite to the suppression effect observed in the CV study (Figure 1). It is possibly because the concentration of $H^+$ in the electrolyte is much higher in this study, and the side reactions such as HER are expected to be more pronounced than Co deposition. Increasing current density to −4.08, −6.12, and −12.76 mA/cm$^2$ led to increasingly more negative potentials and typical steady-state galvanostatic transients were seen for all of the current densities studied.

Figure 3b shows the same galvanostatic study at a higher pH of 5.67. Same as the case with pH 4.0, the suppression effect on Co deposition with the addition of 300 ppm MPS was observed again at −2.55 mA/cm$^2$. The oscillation emerged at a current density of −3.06 mA/cm$^2$, much lower than −4.08 mA/cm$^2$ for a pH of 4. Despite of the different applied current


https://dx.doi.org/10.1021/acs.jpcc.0c06877
J. Phys. Chem. C 2020, 124, 21608−21616

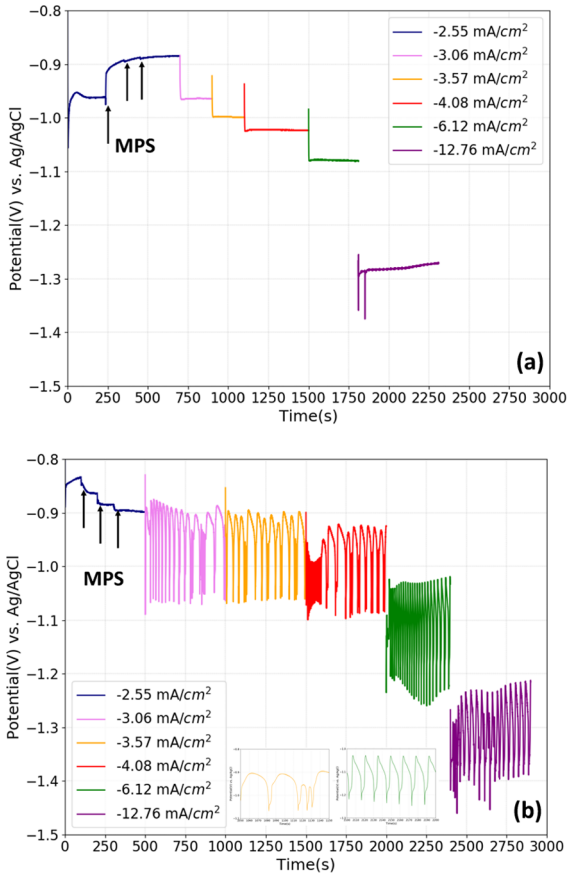


**Figure 3.** Potential transients for Co deposition at 400 rpm and different current densities in 0.05 M Co solutions with the addition of 300 ppm MPS at (a) pH = 3 and (b) pH = 5.67. The detailed oscillation curves at -3.57 and -6.121 mA/cm$^2$ are shown in the inset.

densities, the lower bound (negative) potentials of oscillation were similar between the two cases, indicating that the mechanism of the oscillation process is very likely potential dependent. Based on the magnified oscillation data shown as the inset from 1800 to 1900 s, the oscillation at the same −4.08 mA/cm$^2$ comprised two different modes, full oscillations between −0.9 and −1.1 V and partial oscillations between −1 and −1.1 V. The periods were about 50 and 5 s for the full and partial oscillations, respectively. While such oscillations may seem to be slower than the acidic case (pH = 4 in Figure 2), the oscillations in the latter resembled the partial oscillation mode and were not stable, disappearing completely after only 100 s. Moreover, the oscillations at pH 4 resemble the partial oscillation mode. The partial oscillations disappeared and only full oscillation with a period of 14.3 s was observed as the current density changed from −4.08 to −6.12 mA/cm$^2$. The morphology of a typical film obtained with oscillatory deposition was characterized with SEM and is presented in Figure S-3 in the Supporting Information. A film prepared without MPS or oscillation is included for comparison. Both two films showed a net style morphology or a flake-shaped deposit, however, at different scales. The films prepared with oscillation resulted in larger and probably deeper voids between the flakes. Dense films were obtained in both cases confirmed with cross-sectional characterization. No modulated layer structure was observed in a similar way in Cu, probably related to the fast oscillation.

The observation in Figures 2 and 3 can be summarized as the following. (i) The oscillation phenomenon is potential-dependent and only occurs when the negative potential is below a threshold value. (ii) This threshold potential is necessary but not sufficient for the oscillation and no oscillation can be enabled at a pH of 3 or below. (iii) When an oscillation occurs, this threshold potential seems to be independent of pH. Although different current densities are needed at different pH's to enable the oscillation, the lower bound potentials of the oscillations are similar. (iv) The oscillation period is not only pH dependent but also current dependent. Partial oscillations are often observed at a lower pH or lower current density, with shorter periods or higher frequencies than the full oscillations, and accompanied by a lower upper bound potential. (v) At a pH of 4 or above, a sharp drop followed by a rapid increase of the potential was always observed immediately after the increase of current density.

As mentioned above, Co and MPS could form a complexed adsorbate on the electrode surface. Based on the observations in Figure 3, we hypothesized that the adsorption and desorption of such complex is potential-dependent, favored at less and more negative potentials, respectively. Once a certain negative potential is reached, the desorption of the Co−MPS complex accelerates and its surface coverage decreases, mitigating the suppression effect and resulting in a rise of potential in galvanostatic deposition. Meanwhile, as the potential becomes less negative, the side reactions like proton and water reduction reactions become less active, the pH at the electrode surface decreases, the coverage of the adsorbed $Co(OH)_2$ decreases, and the potential further increases. This forms a positive feedback loop for $Co(OH)_2$ desorption or dissolution triggered by the desorption of the Co−MPS complex. In addition, the incorporation of the Co−MPS complex into the deposit may form another positive feedback itself, as reported for many other systems.[9,14]

Once the majority of the Co−MPS complexes gets incorporated into the deposit and most adsorbed $Co(OH)_2$ are dissolved, the potential reaches a maximum value, corresponding to the upper bound potential in the oscillation. However, the Co−MPS complex in the solution will gradually adsorb and accumulate on the substrate surface, suppressing the deposition of Co and decreasing the potential at a constant current. More importantly, the latter facilitates the side reactions and increases the pH at the electrode surface. Therefore, $Co(OH)_2$ starts to form in the vicinity of the electrode surface, blocking the electrode surface. This, in the same way as above, results in a positive feedback loop of $Co(OH)_2$ adsorption triggered by the adsorption of the Co−MPS complex. The potential gradually decreases in this loop until it reaches a minimum value, or the lower bound potential in the oscillation, which corresponds to a maximum coverage of the Co−MPS complex and $Co(OH)_2$ on the electrode surface. The Co−MPS complex desorption starts at this point, triggering the positive feedback loops of $Co(OH)_2$ desorption and Co−MPS consumption and leading the next cycle of oscillation.

In this hypothesized mechanism, the formation/dissolution of the $Co(OH)_2$ adsorbate is a fast autocatalytic kinetics and the adsorption/desorption of MPS is a relative slow kinetics. The latter is highly potential dependent and serves as the trigger for the oscillation and results in a threshold potential required for the oscillation. On the other hand, the former


https://dx.doi.org/10.1021/acs.jpcc.0c06877
J. Phys. Chem. C 2020, 124, 21608−21616

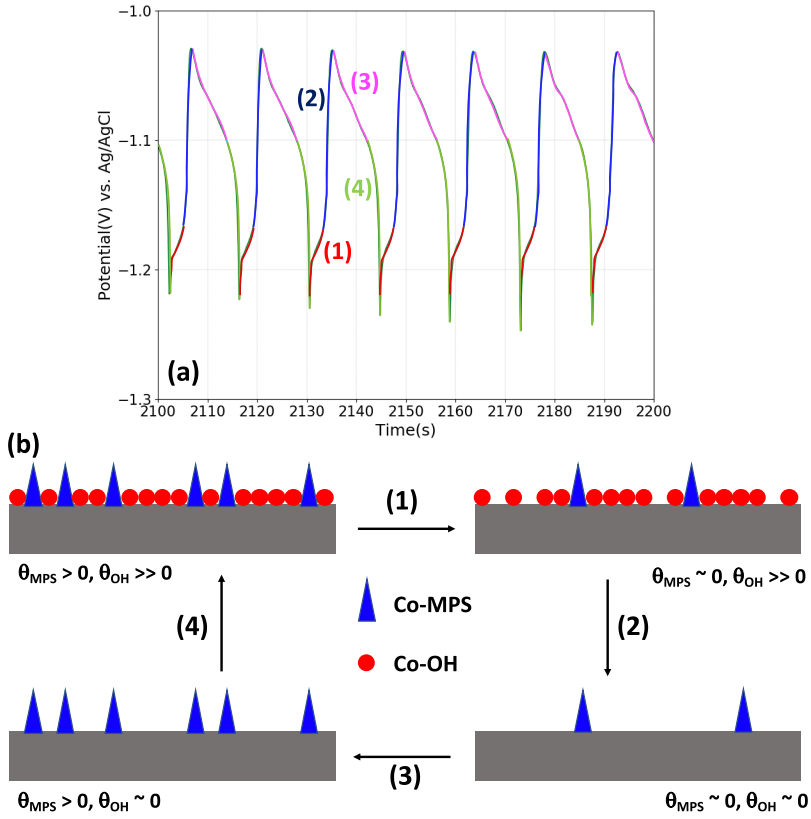


**Figure 4.** (a) Close look of the potential oscillation at 400 rpm and −6.12 mA/cm$^2$ in 0.05 M Co solutions with 300 ppm MPS and pH = 5.67 and (b) diagram showing the four steps of (1) Co−MPS desorption, (2) $Co(OH)_x$ dissolution, (3) Co−MPS adsorption, and (4) $Co(OH)_x$ accumulation.

serves as the main positive feedback and a sufficiently high current density is necessary to drive the reaction rate to be faster than the rate the system equilibrates. When an intermediate current is used, damping oscillations that gradually disappear can occur, depending on the initial condition of the electrode surface. On the other hand, when the electrolyte pH is low, the system equilibrates faster, preventing the emerge of oscillation or resulting in partial oscillations. In addition, the potential range or the magnitude of oscillation highly depends on the surface adsorbate situation or the coverages of the two different adsorbates, which can also depend on the initial coverages and the rate of reaction, i.e., the applied current density.

The unstable oscillation in Figure 2 at −4.08 mA/cm$^2$ is believed to relate to an initial surface coverage off equilibrium. Oscillation emerged driven by the intermediate current and disappeared as the surface coverages readjusted themselves throughout the oscillation and reached a steady-state situation. Again, this steady state was reached because the current was not high enough, allowing sufficient time for the adsorption/desorption of two competitive adsorbates to reach an equilibrium.

A close look at the stable oscillation at −6.12 mA/cm$^2$ in Figure 4a showed that a full oscillation cycle is not symmetrical but composed of several distinct segments. Each rise or drop segment of the potential transients comprises two stages, one slow change followed by a rapid change, consistent with the hypothesized Co−MPS and Co−OH kinetics, respectively. As shown in Figure 4a, while the lower bound voltage varies significantly for each oscillation, the four distinct segments start at much more consistent potentials. The former could result from a nonuniform overformation and precipitation of the $Co(OH)_2$ adsorbate, which however dissolves immediately at certain surface pH. The four distinct potentials suggest that the surface coverage situations are repeatable for each oscillation. As shown in the diagrams in Figure 4b, we here consider that the upper bound potential represents a clean surface free of either adsorbate (or minimum coverage) and the lower bound corresponds a maximum coverage of the mixture between Co−MPS and Co−OH. It is clear that the rapid formation and dissolution of Co−OH are triggered at about −1.10 and −1.19 V, respectively, reflecting the different adsorbate coverages on the electrode. Furthermore, the rise of potential in a cycle is fast, while the drop of potential takes longer time, due to a slower adsorption and faster desorption of the Co−MPS complex. We use the word "desorption" to refer to the decrease of the Co−MPS coverage, but it indeed should include other breakdown mechanisms such as reduction, consumption, or incorporation.

When the applied current decreases, the rate of side reaction, such as the reduction of the proton and water, decreases. Therefore, the formation and adsorption of $Co(OH)_2$ will be slowed, decreasing the oscillation frequency. On the other hand, at a higher current density, the surface concentration of $Co(OH)_2$ is high due to the strong side reactions, which facilitates the adsorption of the $Co(OH)_2$ process and decreases the oscillation period. This explanation is consistent with the experimental results in Figure 3b, where the oscillation period decreases as the current density is changed from −4.08 to −6.12 mA/cm$^2$. It is noted here that we use the period of full oscillation because the partial cycles do not involve the complete breakdown of Co−OH and the


https://dx.doi.org/10.1021/acs.jpcc.0c06877
J. Phys. Chem. C 2020, 124, 21608−21616

adsorption of Co−MPS and the cycles are much faster and not stable.

Based on the hypothesized mechanism, the formation and breakdown of the Co−MPS and Co−OH adsorbates on the electrode surface underpin the oscillations. Therefore, studies are carried out to probe the effects of the constituents of such complexes.

**Influence of $Co^{2+}$ and MPS Concentrations.** Figure 5 shows the galvanostatic study of Co deposition with different concentrations of $Co^{2+}$ and MPS. Figure 5a shows the Co deposition in an electrolyte similar to Figure 3b, with 300 ppm MPS and a natural pH of 5.75, but a higher $Co^{2+}$ concentration of 0.1 M. Similar to the 0.05 M $Co^{2+}$ case, suppression effect was observed with the addition of MPS at −2.55 mA/cm$^2$. However, oscillation did not happen until the current density was increased to −6.12 mA/cm$^2$, much higher than −3.06 mA/cm$^2$ required in the 0.05 M $Co^{2+}$ case. In addition, the oscillation was unstable at −6.12 mA/cm$^2$ and stopped after around 1000 s. Stable oscillations for over 1000 s were achieved at a higher current density of −12.76 mA/cm$^2$. These observations are consistent with a lower effective current density of side reactions due to the increased concentration of the metal ion, namely, a lower driving current for the Co−OH positive feedback loop. The detailed oscillation curves are shown as the inset in Figure 5a. The oscillations resemble the partial oscillation mode observed at lower current densities in Figure 3b, and this is also consistent with the lower effective driving current due to the higher concentration of $Co^{2+}$.

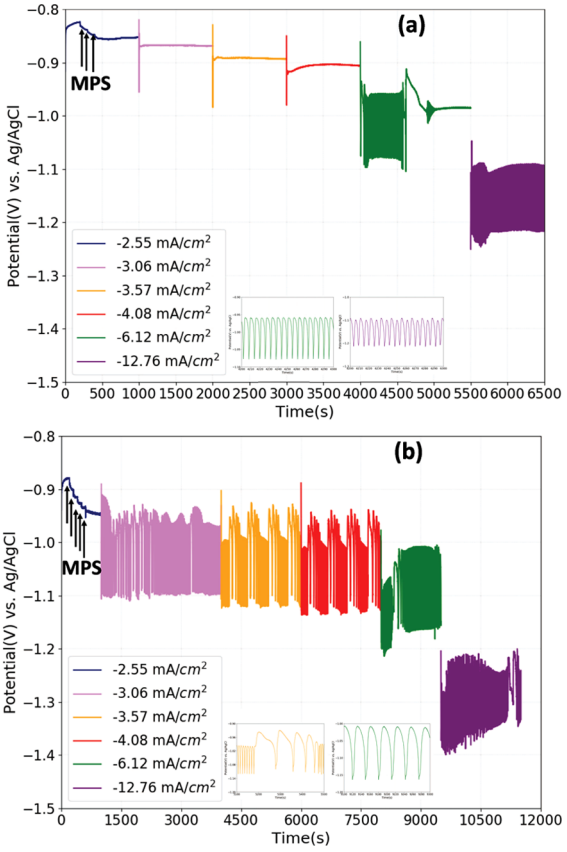


**Figure 5.** Potential transients for Co deposition at 400 rpm and different current densities in (a) 0.1 M Co solutions with the addition of 300 ppm MPS at measured pH = 5.75 and (b) 0.05 M Co solutions with the addition of 500 ppm MPS at pH = 5.67. The detailed oscillation curves are shown in the inset.

The effect of MPS concentration was studied with an electrolyte similar to Figure 3b, with 0.05 M $Co^{2+}$ and a pH of 5.67, but a higher MPS concentration of 500 ppm. The potential transients are shown in Figure 5b. Oscillations with partial mode started at −3.06 mA/cm$^2$, similar to the 300 ppm MPS case. The transformation from partial oscillation to full oscillation started at −3.57 mA/cm$^2$. Stable oscillation was achieved at −6.12 mA/cm$^2$. Comparison between Figure 4 and the inset in Figure 5b at a same current density of −6.12 mA/cm$^2$ clearly shows that the Co−MPS adsorption segment is much less distinctive at higher MPS concentration. This is consistent with the expectation that higher MPS concentration facilitates the adsorption of Co−MPS during the dissolution/desorption of $Co(OH)_2$, disabling a completely adsorbate free surface to be achieved or resulting in a higher minimum surface coverage.

**Influence of Rotation.** Another way of probing the electrode kinetics is to change the agitation, namely, the supply rate of chemical species toward the electrode. Figure 6 shows the oscillatory transients with the disk electrode at various rotation rates. The studies were also carried out in an electrolyte same as Figure 3b, i.e., with 50 mM $Co^{2+}$, 300 ppm MPS, and a pH of 5.67. A fixed current density of −6.12 mA/cm$^2$ was used. These conditions were used because stable oscillations could be achieved at 400 rpm. Different rotation rates from 0 to 1600 rpm were used over a course of 7000 s deposition, and each rotation rate was maintained for enough time till stable oscillations were observed. The stable oscillations for each rotation rate were cropped together and are shown in Figure 6. Stable oscillations with four distinct segments were observed for all rotation rates beyond 0 rpm. The potential range of oscillation seemed to be similar until the rotation rates were below 100 rpm, consistent with the constant current used and the hypothesized mechanism. The lower boundary of the oscillation varied and was consistently more negative at low rotation rates. This is believed to be consistent with the hypothesized mechanism, where the formation and precipitation of Co−OH is expected to be less controlled and more likely to run over the equilibrium at low rotation rates, leading to a more negative potential overshoot.

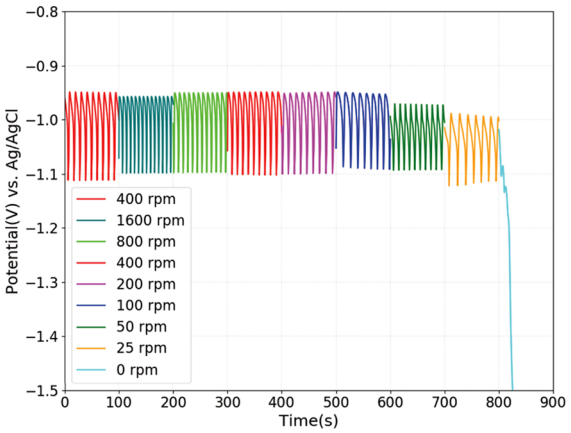


**Figure 6.** Potential transients for Co deposition at different rotation rates in 0.05 M Co solutions with the addition of 300 ppm MPS at pH = 5.67. The applied current density is −6.12 mA/cm$^2$.



https://dx.doi.org/10.1021/acs.jpcc.0c06877
J. Phys. Chem. C 2020, 124, 21608−21616

The average periods for the stable oscillations at different rotation rates were obtained by counting the total time of 10 oscillations and are summarized in Table 1. The rotation rate

**Table 1. Oscillatory Periods at the Different Rotation Rates Obtained from the Potential Transients Shown in Figure 6**

| rotation rate (rpm) | cycles per 100 s | oscillation period (s/cycle) |
|---|---|---|
| 400 | 10 | 10.0 |
| 1600 | 14 | 7.1 |
| 800 | 11 | 9.1 |
| 400 | 10 | 10.0 |
| 200 | 9 | 11.1 |
| 100 | 8 | 12.5 |
| 50 | 10 | 10.0 |
| 25 | 7 | 14.3 |
| 0 | 0 | infinity (no oscillation) |

of 400 rpm was used multiple times during the experiment as a control experiment and the period was found reproducible and independent of the experimental sequence or electrode history. In general, the stable oscillations seemed to be slightly faster at a higher rotation rate, with the period dropped from 14 s at 25 rpm to 7 s at 1600 rpm. While this correlation suggests that mass transport plays a role in the oscillation process, the effect is not strong. The period merely decreased into half with the rotation rates increased by 64 times. It is interesting to find that the main reason for the increase of period was due to the slowdown of the slow kinetic segments, while the fast kinetics or the sharp potential change remained sharp. This is consistent with the hypothesized mechanism as well, where the sharp change is hypothesized to result from a positive feedback of Co−OH formation and dissolution. This process highly relies on the surface pH change, which is expected to be more pronounced as rotation decreases. That is, this rapid positive feedback is not expected to be mitigated at the low rotation rates. On the other hand, the slow kinetics, which is hypothesized to be the adsorption and desorption of the Co−MPS complex, is expected to relate to the surface concentration of such complex and, therefore, the rotation rates. As the rotation rate decreases, the supply of Co−MPS to the electrode or the dilution from the electrode surface slows down, resulting in a slower adsorption or desorption. However, when the agitation is completely stopped, the surface concentrations of all species can be drastically different from the bulk electrolyte. As the metal ion is depleted, side reactions dominate, surface pH increases indefinitely, the surface is completely blocked by the Co−OH complex. The potential decreases to extremely negative values to enable water reduction on this completely blocked electrode, and, of course, oscillation completely ceases.

**Influence of $H_3BO_3$.** To further test the role of surface pH in oscillation, we conducted another study on the effect of a pH buffer, $H_3BO_3$. An electrolyte similar to Figure 3b, with 0.05 M $Co^{2+}$ and 300 ppm MPS, was used. But the pH was changed from 5.67 to 4.3 upon the addition of 0.4 M $H_3BO_3$. As discussed in Figures 2 and 3, the electrolytes without boric acid at pH of 4 and 5.67 both showed oscillation, albeit starting at different current densities. Therefore, this different bulk pH of 4.3 was not expected to cause a significant change in oscillation. The potential transients at different current densities in this buffered electrolyte are presented in Figure 7. Not only were oscillations not observed regardless of the

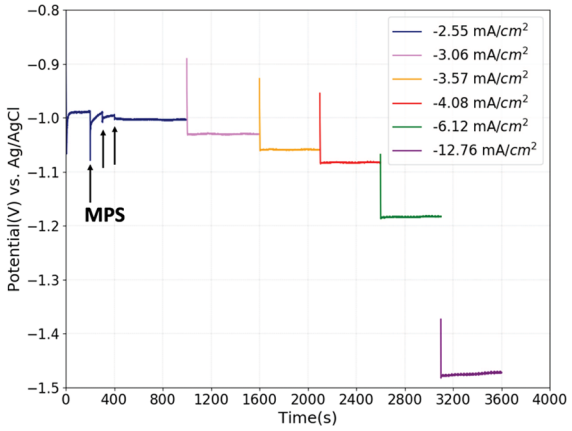


**Figure 7.** Potential transients for Co deposition at 400 rpm and different current densities in 0.05 M Co solutions with the addition of 300 ppm MPS and 0.4 M $H_3BO_3$ at measured pH = 4.3.

current densities, but also less negative overall deposition potentials were resulted. Such observations are similar to the pH = 3 case in Figure 3a. Boric acid is a pH buffer with a $pK_a$ of 9.24, commonly used in iron-group magnetic alloy electrodeposition to prevent extremely high pH and hydroxide incorporation in the films.[31] The absence of oscillation here further confirms that a high surface pH and the formation of $Co(OH)_2$ play an important role in the oscillation.

**Influence of Mercaptopropionic Acid.** To further understand the structure of the $Co^{2+}$−MPS complex, mercaptopropionic acid, or MPA, an acid with a similar structure as MPS, was used in place of MPS. The only structural difference between the two is that MPS contains the sulfonate group and MPA contains the carboxyl group. Figure 8 shows the potential transients with the addition of 300 ppm

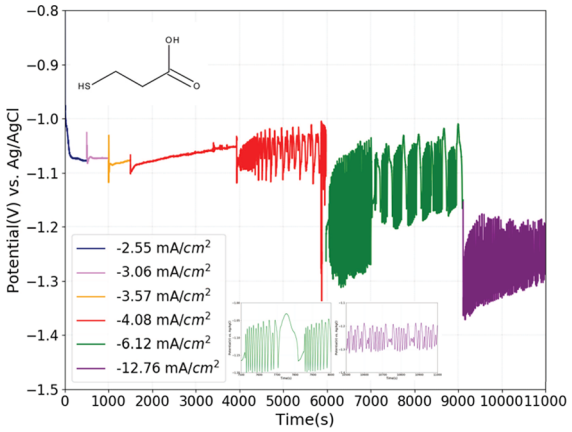


**Figure 8.** Potential transients for Co deposition at different current densities in 0.05 M Co solutions with the addition of 300 ppm MPA at adjusted pH = 5.67.

MPA in the 0.05 M $Co^{2+}$ electrolyte. While the addition of 300 ppm MPA significantly decreased the solution pH from 5.67 to around 3.76, pH was readjusted back to 5.67 prior to the galvanostatic deposition study. The $pK_a$ of the carboxyl group is 4.6,[32] and no buffering is expected from this carboxyl group in this electrolyte with the pH of 5.67. The oscillation was observed at −4.08 mA/cm$^2$, but only after the current was applied for nearly 2500 s. As shown in the inset, the oscillation was not stable and partial oscillations were also observed,


https://dx.doi.org/10.1021/acs.jpcc.0c06877
J. Phys. Chem. C 2020, 124, 21608−21616

where the lower bound potential or the maximum surface coverage by Co−OH was not fully reached. Further increasing the current density did not lead to stable oscillation. Since the formation of the complex is important for the oscillation behavior, this experiment result confirms that Co will interact with the thiol group to form the Co−MPS or Co−MPA complex on the electrode surface. The CVs of MPA are provided in Figure S-4 in the Supporting Information, where a stronger suppression effect was observed for MPA than MPS. This is also consistent with the fact that MPA has an additional carboxyl group which, in conjunction with the thiol group, prefers to chelate with the bivalent $Co^{2+}$ to form a more stable complex Co−$(MPA)_2$ with a stability constant around 13.[32] This stronger suppressive adsorbate apparently not only drives the deposition potential to a more negative range but also alters the competitive surface coverage and the oscillation behavior.

## CONCLUSIONS

A potential oscillation was observed during galvanostatic deposition of Co in the presence of MPS, which mildly suppressed the deposition. The fast autocatalytic kinetics of the accumulation and dissolution of $Co(OH)_2$ were proposed as the main positive feedback loops for this oscillation, which were, respectively, triggered by the slow but potential-dependent adsorption and desorption of the Co−MPS complex. This mechanism was verified by a systematic study on the effects of the parameters including bulk pH, $Co^{2+}$ and MPS concentration, rotation rate, and pH buffer. In addition, oscillation was also observed when an alternative additive, MPA, was used, confirming the formation of the Co−MPS complex through the thiol group and the critical role such complex played in the oscillation.

## ASSOCIATED CONTENT

### Supporting Information

The Supporting Information is available free of charge at https://pubs.acs.org/doi/10.1021/acs.jpcc.0c06877.

Cyclic voltammetry of Co electrodeposition on Pt RDE with different MPS concentrations at different pH; electrochemical impedance spectra of Co deposition with different MPS concentrations at pH = 3; top-down SEM micrographs of the electrodeposited cobalt films; cyclic voltammetry of Co electrodeposition on Pt RDE with 300 ppm MPA concentrations (PDF)

## AUTHOR INFORMATION


### Corresponding Author

**Q. Huang** − *Department of Chemical and Biological Engineering, University of Alabama, Tuscaloosa, Alabama 35487, United States;* orcid.org/0000-0002-1391-6531; Email: qhuang@eng.ua.edu

### Author

**Y. Hu** − *Department of Chemical and Biological Engineering, University of Alabama, Tuscaloosa, Alabama 35487, United States;* orcid.org/0000-0002-8943-2584

Complete contact information is available at: https://pubs.acs.org/10.1021/acs.jpcc.0c06877


### Notes

The authors declare no competing financial interest.

## ACKNOWLEDGMENTS

National Science Foundation is acknowledged for the support through Grant CMMI-1662332. Y.H. thanks the Graduate Council at the University of Alabama for a fellowship support. The Central Analytical Facility at the University of Alabama is acknowledged for the access of equipment for characterization.

## REFERENCES


(1) Steinhögl, W.; Schindler, G.; Steinlesberger, G.; Engelhardt, M. Size-dependent resistivity of metallic wires in the mesoscopic range. *Phys. Rev. B: Condens. Matter Mater. Phys.* **2002**, *66*, No. 075414.

(2) He, M.; Zhang, X.; Nogami, T.; Lin, X.; Kelly, J.; Kim, H.; Spooner, T.; Edelstein, D.; Zhao, L. Mechanism of Co liner as enhancement layer for Cu interconnect gap-fill. *J. Electrochem. Soc.* **2013**, *160*, D3040−D3044.

(3) Wu, W.; Brongersma, S.; Van Hove, M.; Maex, K. Influence of surface and grain-boundary scattering on the resistivity of copper in reduced dimensions. *Appl. Phys. Lett.* **2004**, *84*, 2838−2840.

(4) Gall, D. Electron mean free path in elemental metals. *J. Appl. Phys.* **2016**, *119*, No. 085101.

(5) Moffat, T.; Wheeler, D.; Huber, W.; Josell, D. Superconformal electrodeposition of copper. *Electrochem. Solid-State Lett.* **2001**, *4*, C26−C29.

(6) Huang, Q.; Avekians, A.; Ahmed, S.; Parks, C.; Baker-O'Neal, B.; Kitayaporn, S.; Sahin, A.; Sun, Y.; Cheng, T. Impurities in the electroplated sub-50 nm Cu lines: The effects of the plating additives. *J. Electrochem. Soc.* **2014**, *161*, D388−D394.

(7) Kelly, J.; Nogami, T.; Van der Straten, O.; Demarest, J.; Li, J.; Penny, C.; Vo, T.; Parks, C.; DeHaven, P.; Hu, C.-K.; Liniger, E. Electrolyte additive chemistry and feature size-dependent impurity incorporation for Cu interconnects. *J. Electrochem. Soc.* **2012**, *159*, D563−D569.

(8) Moffat, T. P.; Wheeler, D.; Kim, S.-K.; Josell, D. Curvature enhanced adsorbate coverage model for electrodeposition. *J. Electrochem. Soc.* **2006**, *153*, C127−C132.

(9) Hai, N.; Furrer, J.; Gjuroski, I.; Bircher, M.; Cascella, M.; Broekmann, P. On the Acceleration of Cu Electrodeposition by TBPS (3, 3-thiobis-1-propanesulfonic acid): A Combined Electrochemical, STM, NMR, ESI-MS and DFT Study. *J. Electrochem. Soc.* **2013**, *160*, D3158.

(10) Chiu, Y.-D.; Dow, W.-P.; Krug, K.; Liu, Y.-F.; Lee, Y.-L.; Yau, S.-L. Adsorption and desorption of Bis-(3-sulfopropyl) disulfide during Cu electrodeposition and stripping at Au electrodes. *Langmuir* **2012**, *28*, 14476−14487.

(11) Walker, M. L.; Richter, L. J.; Moffat, T. P. Competitive adsorption of PEG, Cl−, and SPS/MPS on Cu: an in situ ellipsometric study. *J. Electrochem. Soc.* **2006**, *153*, C557−C561.

(12) Moffat, T. P.; Wheeler, D.; Josell, D. Electrodeposition of copper in the SPS-PEG-Cl additive system I. Kinetic measurements: Influence of SPS. *J. Electrochem. Soc.* **2004**, *151*, C262−C271.

(13) Orban, M.; Epstein, I. R. Oscillations and bistability in hydrogen-platinum-oxyhalogen systems. *J. Am. Chem. Soc.* **1981**, *103*, 3723−3727.

(14) Hai, N. T.; Odermatt, J.; Grimaudo, V.; Krämer, K. W.; Fluegel, A.; Arnold, M.; Mayer, D.; Broekmann, P. Potential oscillations in galvanostatic Cu electrodeposition: antagonistic and synergistic effects among SPS, chloride, and suppressor additives. *J. Phys. Chem. C* **2012**, *116*, 6913−6924.

(15) Bohannan, E. W.; Huang, L.-Y.; Miller, F. S.; Shumsky, M. G.; Switzer, J. A. In situ electrochemical quartz crystal microbalance study of potential oscillations during the electrodeposition of Cu/Cu2O layered nanostructures. *Langmuir* **1999**, *15*, 813−818.

(16) Strasser, P.; Eiswirth, M.; Ertl, G. Oscillatory instabilities during formic acid oxidation on Pt (100), Pt (110) and Pt (111) under potentiostatic control. II. Model calculations. *J. Chem. Phys.* **1997**, *107*, 991−1003.

(17) Strasser, P.; Lübke, M.; Raspel, F.; Eiswirth, M.; Ertl, G. Oscillatory instabilities during formic acid oxidation on Pt (100), Pt

(110) and Pt (111) under potentiostatic control. I. Experimental. *J. Chem. Phys.* **1997**, *107*, 979−990.
(18) Strasser, P.; Eiswirth, M.; Koper, M. T. Mechanistic classification of electrochemical oscillators—an operational experimental strategy. *J. Electroanal. Chem.* **1999**, *478*, 50−66.
(19) Hai, N. T.; Krämer, K. W.; Fluegel, A.; Arnold, M.; Mayer, D.; Broekmann, P. Beyond interfacial anion/cation pairing: The role of Cu (I) coordination chemistry in additive-controlled copper plating. *Electrochim. Acta* **2012**, *83*, 367−375.
(20) Hai, N.; Furrer, J.; Barletta, E.; Lüdi, N.; Broekmann, P. Copolymers of imidazole and 1, 4-butandiol diglycidyl ether as an efficient suppressor additive for copper electroplating. *J. Electrochem. Soc.* **2014**, *161*, D381−D387.
(21) Barkey, D.; Chang, R.; Liu, D.; Chen, J. Observation of a limit cycle in potential oscillations during copper electrodeposition in a leveler/accelerant system. *J. Electrochem. Soc.* **2014**, *161*, D97−D101.
(22) Switzer, J. A.; Hung, C.-J.; Huang, L.-Y.; Miller, F. S.; Zhou, Y.; Raub, E. R.; Shumsky, M. G.; Bohannan, E. W. Potential oscillations during the electrochemical self-assembly of copper/cuprous oxide layered nanostructures. *J. Mater. Res.* **1998**, *13*, 909−916.
(23) Leopold, S.; Herranen, M.; Carlsson, J.-O. Spontaneous potential oscillations in the Cu (II)/tartrate and lactate systems, aspects of mechanisms and film deposition. *J. Electrochem. Soc.* **2001**, *148*, C513−C517.
(24) Huang, X.-P.; Han, W.; Shi, Z.-L.; Wu, D.; Wang, M.; Peng, R.-W.; Ming, N.-B. Electrodeposition of periodically nanostructured straight cobalt filament arrays. *J. Phys. Chem. C* **2009**, *113*, 1694−1697.
(25) Huang, Q.; Lyons, T.; Sides, W. Electrodeposition of Cobalt for Interconnect Application: Effect of Dimethylglyoxime. *J. Electrochem. Soc.* **2016**, *163*, D715−D721.
(26) Lyons, T.; Huang, Q. Effects of Cyclohexane-Monoxime and Dioxime on the Electrodeposition of Cobalt. *Electrochim. Acta* **2017**, *245*, 309−317.
(27) Hu, Y.; Huang, Q. Effects of Dimethylglyoxime and Cyclohexane Dioxime on the Electrochemical Nucleation and Growth of Cobalt. *J. Electrochem. Soc.* **2019**, *166*, D3175−D3181.
(28) Caruso, A.; Wang, L.; Jaswal, S.; Tsymbal, E. Y.; Dowben, P. A. The interface electronic structure of thiol terminated molecules on cobalt and gold surfaces. *J. Mater. Sci.* **2006**, *41*, 6198−6206.
(29) Hu, Y.; Huang, Q. Thermal Annealing and Impurities Incorporation of Electrodeposited Cobalt Thin Film. In *ECS Meeting Abstracts*; The Electrochemical Society, 2019; pp 1256.
(30) Santos, J.; Trivinho-Strixino, F.; Pereira, E. Investigation of Co (OH) 2 formation during cobalt electrodeposition using a chemometric procedure. *Surf. Coat. Technol.* **2010**, *205*, 2585−2589.
(31) Andricacos, P.; Arana, C.; Tabib, J.; Dukovic, J.; Romankiw, L. Electrodeposition of Nickel-Iron Alloys: I. Effect of Agitation. *J. Electrochem. Soc.* **1989**, *136*, 1336.
(32) Martell, A. E.; Smith, R. M. *Critical Stability Constants*; Springer, 1974; Vol. *1*.


https://dx.doi.org/10.1021/acs.jpcc.0c06877
*J. Phys. Chem. C* 2020, 124, 21608−21616